A New Edge Element for the Modeling of Field Singularities in Transmission Lines and Waveguides

José M[a] Gil and Jon P. Webb, *Member, IEEE*

***Abstract*—Edge finite elements are widely used in the analysis of waveguides and transmission lines. They have tangential continuity and they do not produce spurious modes. However, they cannot model the singular behavior of the transverse fields in the neighborhood of sharp edges. This fact limits the accuracy of the representation of the fields and the order of convergence of the method. In this paper, we present a new edge element in which the singular approximation of the three fields components and the correct modeling of the curl is incorporated. The development of the basis functions is described. Some numerical results for waveguides with sharp metal edges are shown in order to validate this theory.**

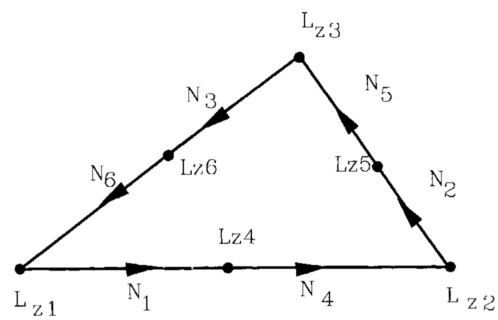

Fig. 1. The new singular-edge element.

I. Introduction

The presence of field singularities in many common transmission lines and waveguides has led to several publications over the last few years, which have focused on the improvement of the convergence and approximation of the unknown function in the finite-element method (FEM). In the scalar case (quasi-TEM analysis of transmission lines and homogeneous waveguide analysis) special finite elements—called singular elements—have been developed [1], [2].

In the case of full-wave analysis, a nodal element with singular approximation of transverse-field components was presented in [3]. Edge elements, which avoid the problem of the continuity of the transverse component on sharp edges and remove the spurious modes, have been quickly adopted by the users of the FEM. However, these elements do not properly model the singular field because they use polynomials as basis functions [4]. When the problem to be analyzed has singularities, the order of convergence is very poor and the transversal fields in the singular zones are not accurately computed.

In [5], a new edge element with singular approximation of the fields was presented. The relative complexity of this element and the lack of results published to date have justified the search for another solution.

Manuscript received January 14, 1997; revised August 22, 1997. This work was supported by the DGICYT of the Ministerio de Educación y Ciencia of Spain, by the CICYT under contract TIC95-0137-C02-01, and by the Natural Sciences and Engineering Research Council of Canada.

J. M. Gil is with the Departamento de Electromagnetismo y Teoría de Circuitos, Escuela Técnica Superior de Ingenieros de Telecomunicación, Universidad Politécnica de Madrid, Ciudad Universitaria 28040 Madrid, Spain.

J. P. Webb is with the Department of Electrical Engineering, McGill University, Montreal, P.Q., Canada H3A 2A7.

Publisher Item Identifier S 0018-9480(97)08245-8.

This paper introduces a singular-edge element with a correct approximation of the singular transverse-field component as well as the axial component, according to Meixner's theory [6]. The curl of the transversal field is also adequately modeled. The result is an element which can easily be incorporated in a standard finite-element code and has important improvements over other methods with regard to the convergence and approximation of fields.

Some common waveguides with sharp metal edges are analyzed in order to check the improvement achieved by using the new element.

II. The New Edge Element

The new edge element is an hybrid nodal/edge element with six tangential unknowns associated with the edges, and six axial unknowns associated with the vertices and midpoint node of the edges (see Fig. 1). For the electric field, the transverse component E_t is approximated by using vectorial shape functions and the axial component E_z by scalar shape functions (the same is true for the magnetic field).

A. Behavior of Field Components in the Neighborhood of Sharp Edges

It is known that in the neighborhood of an edge, the field components have the following behavior:

$$E_t \to r^{\nu-1} \quad E_z \to r^{\nu} \quad 0 < \nu < 1 \tag{1}$$

where r is the radial distance from the edge and ν is the order of the singularity [6].

The singular field, in a small area around the singularity, is considered to be a static field. The dynamic component is

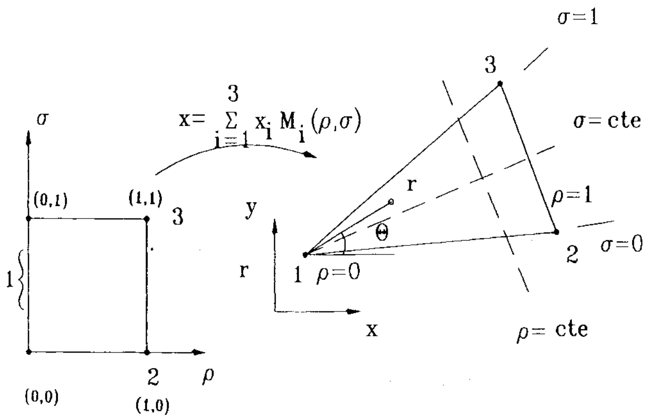

Fig. 2. Mapping of new element.

regular. On the other hand, the behavior of the transverse curl must be

$$\nabla_{tx}\vec{E}_t \rightarrow r^{\nu}. \tag{2}$$

These singular behaviors are represented by approximating the unknown function in the following way.

B. Geometric Transformation

We begin by describing the geometric transformation employed to move the approximation of the field from local to real space $(x,\, y)$.

The elements of the mesh in real space are mapped into the reference element (unit square) by means of the following transformation (see Fig. 2):

$$t - t_1 = \rho[(t_2 - t_1) + (t_3 - t_2)\sigma], \qquad t = x,\, y \tag{3}$$

where $t_i,\ i = 1, 2, 3$ are the coordinates of the vertices of the element, and $\rho,\, \sigma$ are the triangular polar coordinates.

It can be seen that at the point $\rho = 0$, the Jacobian vanishes and the transformation is not invertible at this point. The straight lines defined by $\sigma =$ constant are converted to straight lines passing through vertex one.

By studying this geometrical transformation, we can make the following conclusions:

$$\begin{aligned} r &= R(\sigma)\rho \\ \theta &= \Theta(\sigma) \end{aligned} \tag{4}$$

where $(r,\, \theta)$ are cylindrical polar coordinates centered on vertex one. We can see that radial distances in real and local spaces are proportional and, therefore, along any radial direction $\sigma =$ constant, passing through the singular point (vertex one), the singular behavior given by (1) and (2) becomes

$$\begin{aligned} E_t &\rightarrow \rho^{\nu-1} \\ E_z &\rightarrow \rho^{\nu} \\ \nabla_{tx}\vec{E}_t &\rightarrow \rho^{\nu}. \end{aligned} \tag{5}$$

In order to do the integration in the unit square, a 16-point quadrature formula has been employed. We have found that this order of integration is enough to get satisfactory results. The integrals which appear in the formulation could also be done in closed form with the help of a conventional symbolic mathematics program, but this option is complicated and it ruins the simplicity with which the new element can be incorporated in a standard finite-element code.

C. Approximation of the Transverse Component of the Unknown Function

The transverse field is approximated in the form

$$\begin{aligned} \vec{E}_t &= \vec{E}_{t_{\text{reg}}} + \vec{E}_{t_{\text{sing}}} \\ \vec{E}_{t_{\text{reg}}} &= \sum_{i=1}^{3} E_i \vec{N}_i(\rho,\, \sigma) \\ \vec{E}_{t_{\text{sing}}} &= \sum_{i=4}^{6} E_i \vec{N}_i(\rho,\, \sigma) \end{aligned} \tag{6}$$

where $\rho,\, \sigma$ are triangular polar coordinates (see Fig. 2). In the following, we show how the basis functions N_i are built.

The simplex or baricentric coordinates for a triangle are L_1, L_2, and L_3. They are related to $\rho,\, \sigma$ as follows:

$$L_1 = 1 - \rho \quad L_2 = \rho(1 - \sigma) \quad L_3 = \rho\sigma. \tag{7}$$

Starting from these, we build the following vector basis functions:

$$\begin{aligned} \vec{N}_1 &= L_1\nabla L_2 - L_2\nabla L_1 = (1 - \sigma)\nabla\rho + \rho(\rho - 1)\nabla\sigma \\ \vec{N}_2 &= L_2\nabla L_3 - L_3\nabla L_2 = \rho^2\nabla\sigma \\ \vec{N}_3 &= L_3\nabla L_1 - L_1\nabla L_3 = -\sigma\nabla\rho + \rho(\rho - 1)\nabla\sigma. \end{aligned} \tag{8}$$

The approximation of the regular term (dynamic component) then corresponds to an ordinary Whitney element [7]. It contributes a curl which is constant.

For the singular term, three degrees of freedom (one on each edge) are added to the Whitney element. To do this, we define

$$\begin{aligned} L_1^s &= 1 - \rho^{\nu-1} \\ L_2^s &= \rho(1 - \sigma) \\ L_3^s &= \rho\sigma \end{aligned} \tag{9}$$

and we build the two following functions:

$$\begin{aligned} \vec{N}_4 &= \nabla(L_1^s L_2^s) = (1 - \sigma)(1 - \nu\rho^{\nu-1})\nabla\rho + (\rho^{\nu} - \rho)\nabla\sigma \\ \vec{N}_6 &= \nabla(L_1^s L_3^s) = \sigma(1 - \nu\rho^{\nu-1})\nabla\rho + (\rho - \rho^{\nu})\nabla\sigma. \end{aligned} \tag{10}$$

In this way, the singular term (5) in the approximation of the transverse component (static term) is incorporated, as can be seen. It is also obvious that these functions are irrotational and, therefore, they do not contribute any term to the curl. In order to obtain the corresponding approximation of the transverse component of the curl, the basis is completed with

$$\vec{N}_5 = \rho^{\nu+2}(1 - 2\sigma)\nabla\sigma. \tag{11}$$

It is easy to prove that

$$\nabla \times \vec{N}_5 = C\rho^{\nu}(1 - 2\sigma)\vec{z} \tag{12}$$

where C is a constant, then obtaining the expected behavior (5).

By observing the $\vec{N}_i$ functions, we can see that each has only a tangential component along its own edge, but not along the other edges. The tangential continuity between the elements can be easily achieved by matching the parameters E_i in the usual way. It can also be seen that if we associate the vertex one with the singular point, we obtain an element that is compatible with regular (fully first-order) edge elements, adjacent to the edge opposite vertex one. In fact, along this edge ($\rho = 1$) we have

$$\vec{E}_t(\rho = 1) = [E_2 + E_5(1 - 2\sigma)]\nabla\sigma \tag{13}$$

which has the same σ variation as a regular fully first-order element.

D. Approximation of the Longitudinal Component of the Unknown Function

A nodal approximation supported by the vertex and the midpoint node of the edges, is enough to approximate the axial component. However, we again need to incorporate the variation predicted by the theory (1). This is achieved by using the following six-node scalar singular element described in [8]. In this element, the axial-field component is approximated by means of the following:

$$E_z = \sum_{i=1}^{6} E_{z_i} L_{z_i}(\rho, \sigma) \tag{14}$$

$$\begin{aligned}
L_{z_1}(\rho, \sigma) &= 1 + \frac{1}{\beta - 1}\left[\rho(2 - \beta) - \rho^\nu\right]\\
L_{z_2}(\rho, \sigma) &= (1 - \sigma)\left[\frac{\rho\beta}{\beta - 1} - \rho^\nu\left(\frac{1}{\beta - 1} + 2\sigma\right)\right]\\
L_{z_3}(\rho, \sigma) &= \sigma\left\{\frac{\rho\beta}{\beta - 1} - \rho^\nu\left[\frac{1}{\beta - 1} + 2(1 - \sigma)\right]\right\}\\
L_{z_4}(\rho, \sigma) &= \frac{2(1 - \sigma)}{\beta - 1}\left(\rho^\nu - \rho\right)\\
L_{z_5}(\rho, \sigma) &= 4\rho^\nu\sigma(1 - \sigma)\\
L_{z_6}(\rho, \sigma) &= \frac{2\sigma}{\beta - 1}\left(\rho^\nu - \rho\right)\\
\beta &= 2^{(1-\nu)}.
\end{aligned} \tag{15}$$

It is easy to demonstrate that the unknown function is approximated as follows:

$$u_h(\rho, \sigma) = P(\sigma)\rho^\nu + Q(\rho, \sigma) \tag{16}$$

where P and Q are polynomials.

The radial gradient is

$$\frac{\partial E_z}{\partial r} = a_1(\sigma) + \nu a_2(\sigma)\rho^{\nu-1}. \tag{17}$$

In this way, the longitudinal component of field and its gradient are properly modeled. Along the edge opposite to vertex one, this element is compatible with the Lagrange quadratic elements.

In summary, the developed element has the following characteristics: singular approximation of the three field components according to the Meixner's theory for any order of singularity, tangential continuity along the edges of the element allowing for the discontinuity of normal components, compatibility with standard edge elements along the edge opposite to the singularity, adequate modeling of the curl, and removal of spurious modes.

III. Some Numerical Results

In order to check the behavior of the new element we discretize the classical functional

$$F_E = \int_\Omega (\nabla x\vec{E})^* \,[\mu_r]^{-1}(\nabla x\vec{E})\, d\Omega - k_o^2 \int_\Omega \vec{E}^* \,[\varepsilon_r]\, \vec{E}\, d\Omega \tag{18}$$

in terms of the electric field [9], or

$$F_H = \int_\Omega (\nabla x\vec{H})^* \,[\varepsilon_r]^{-1}(\nabla x\vec{H})\, d\Omega - k_o^2 \int_\Omega \vec{H}^* \,[\mu_r]\, \vec{H}\, d\Omega \tag{19}$$

in terms of the magnetic field [10], where $[\mu_r]$ and $[\varepsilon_r]$ are the relative permeability and permittivity tensors, respectively, Ω is the cross section of the waveguide and k_o is the free-space wavenumber

$$k_o^2 = \omega^2\varepsilon_o\mu_o. \tag{20}$$

We analyze several waveguides with field singularities, comparing the results obtained with the new element and those calculated by using a fully first-order edge element with six degrees of freedom and regular approximation for the transverse component and a six-node Lagrange element for the axial component. When we use a mesh with the new element, the singular point is surrounded by these elements. In each case, the size of the singular elements is chosen to be much smaller than the cutoff wavelength of the mode we are studying.

A. Rectangular Vaned Waveguide

The cross section is given in Fig. 3. This structure has a metallic edge which is associated with a singularity of order $\nu = 1/2$. There is a plane of symmetry, but only the modes with a magnetic-wall condition on this plane will be singular. We have calculated the k_o with the phase constant $\beta = 1$ rad/cm, corresponding to the first TE singular mode and then the cutoff wavenumber k_c (20). The convergence of the method by using the new singular elements (four elements surrounding the singularity, the rest regular elements) and by using only regular elements in the mesh has been studied. In order to properly study the convergence, uniform meshes have been employed, and the number of degrees of freedom is increased by means of successive regular refinements of the original mesh. The results for the k_c, by using both E- and H-field are given in Fig. 3. In this figure we can see that by using the new elements, the value of convergence is achieved with much fewer degrees of freedom. This can lead to an important computational economy and a better approximation of divergent transversal fields in the neighborhood of sharp

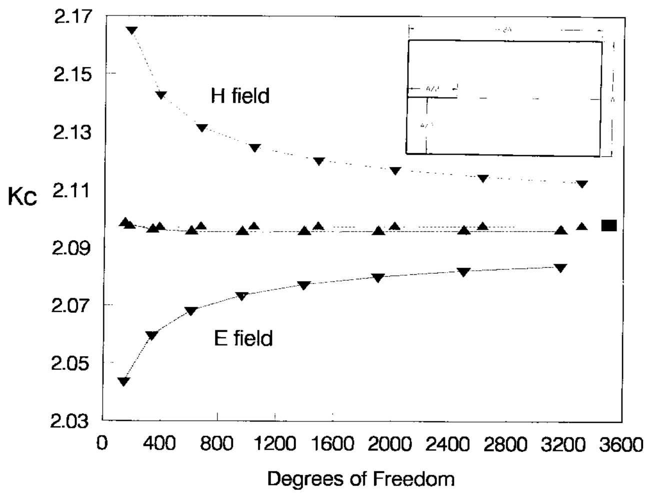

Fig. 3. k_c (rad/cm) of the first singular TE mode, for the rectangular vaned waveguide ($A = 1$ cm), versus the number of degrees of freedom (E- and H-field). ▲: with singular elements. ▼: only regular elements. ■: [2].

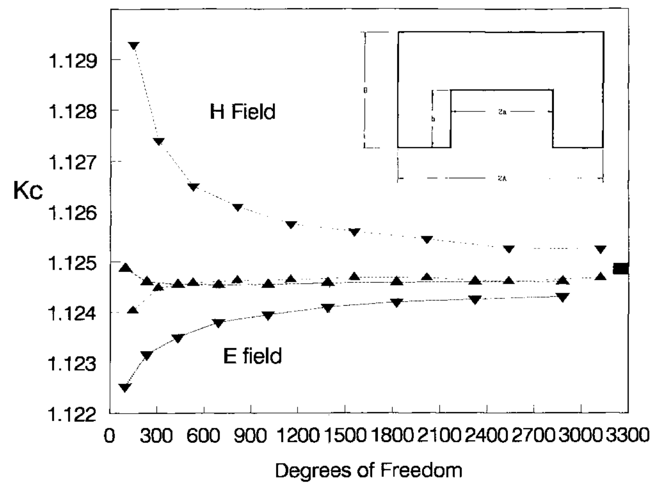

Fig. 5. k_c (rad/cm) of the fundamental mode, for the single-ridge waveguide ($A = B = 0.5$ cm; $a = b = 0.25$ cm), versus the number of degrees of freedom (E- and H-field). ▲: with singular elements. ▼: only regular elements. ■: [2].

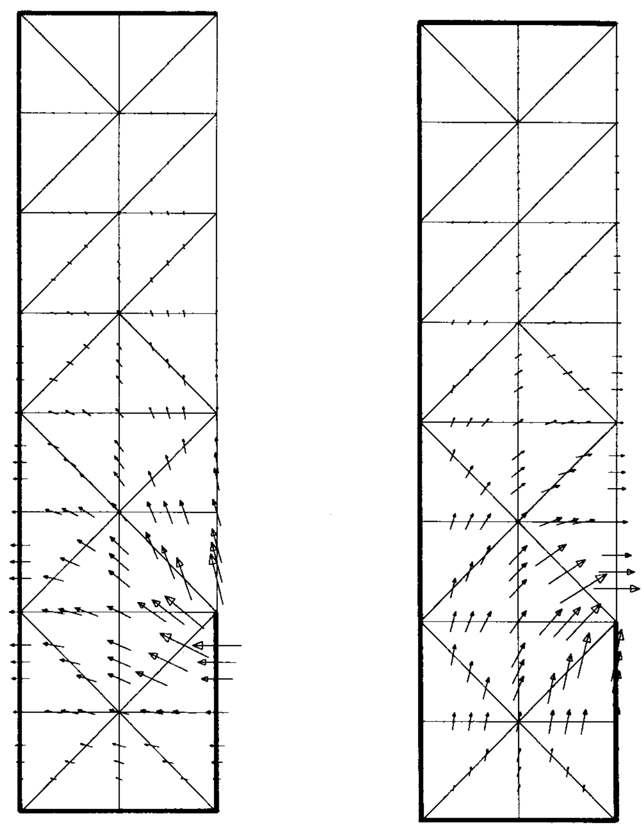

Fig. 4. Transverse electric and magnetic fields, calculated by using four singular elements surrounding the corner (and regular edge elements in the rest) in a mesh with 32 elements.

edges when we use the new elements instead of using the conventional edge elements.

In Fig. 4, we show both transversal electric and magnetic fields calculated by using the singular base functions in four singular elements surrounding the singularity (and with regular functions in the rest) at some points in a mesh of 32 elements. The field just in the corner has not been calculated because it is obviously infinite.

B. Single-Ridge Waveguide

The geometry is given in Fig. 5. The order of singularity is $\lambda = 2/3$ and it has a plane of symmetry; therefore, we analyze one half of the structure. Again, we study the convergence by using regular refinements of uniform meshes. In one series of these meshes, six singular elements surrounding the edge are used and in the other series only regular elements are employed. The mode analyzed was the fundamental (TE). The results for both the E- and H-field can be seen in Fig. 5. It can also be noticed how the value of convergence is achieved much more quickly by using the new elements instead of using regular edge elements.

In Fig. 6, we again show both transversal and electric fields computed from singular functions in six singular elements surrounding the corner (and from regular functions in the rest) in a mesh with 24 elements.

C. Double-Ridge Waveguide

The section is shown in Fig. 7. This structure has been solved by many authors and many different methods. Because of the symmetries, only a quarter of the section is meshed and we again employ meshes with singular elements and with only regular elements. Because of the geometry of this structure, uniform meshes of the section cannot be obtained; therefore, it is not strictly correct to obtain a curve of convergence as in the previous cases. However, by observing the results given in Table I, similar conclusions can be drawn. In this table, k_c for the first three TE modes (E- and H-field) are given by using a different number of degrees of freedom. The comparison between the two types of meshes with the new elements and with only regular elements is obvious from the results in the table. An improvement is achieved when the singular elements are used.

D. Shielded Microstrip Line

In order to show how the elements work when hybrid modes are analyzed, a shielded microstrip line has been studied (see

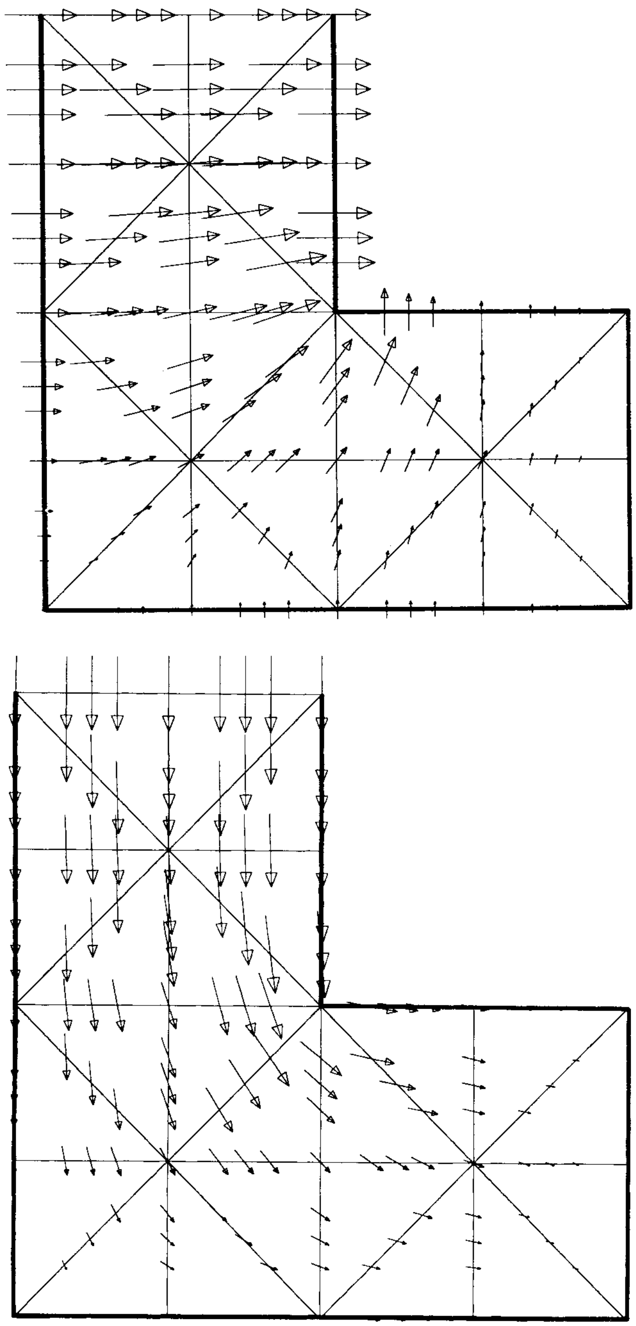

Fig. 6. Transverse electric and magnetic fields calculated by using six singular elements surrounding the corner (and regular edge elements in the rest) in a mesh with 24 elements.

Fig. 8). We analyze one half of the structure, imposing the magnetic-wall condition along the plane of symmetry. The initial mesh was refined to check convergence. Table II gives the results for k_o rad/mm of the dominant mode with the phase constant $\beta = 0.5$ rad/mm and the second mode with $\beta = 1$ rad/mm. We have employed the E formulation in this case. The given results can be compared with those in [12]. Once again, the use of the singular elements speeds convergence and increases accuracy, particularly when relatively few degrees of freedom are used.

In all the cases analyzed, spurious modes have not been detected.

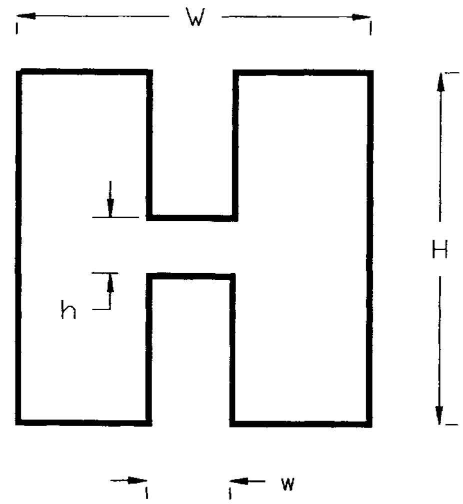

Fig. 7. Double-ridge waveguide. $W = 12.7$ mm, $w = 2.54$ mm, $H = 10.16$ mm, $h = 2.794$ mm.

TABLE I
k_c (RAD/MM) FOR THE FIRST THREE TE MODES
(DOUBLE-RIDGE WAVEGUIDE, E- AND H-FIELD)

D. of F.	REG.	REG.	REG.	SIN.	SIN.	SIN.
E 76	.1424	.6421	.6895	.1431	.6379	.6809
H 124	.1455	.6203	.6730	.1439	.6181	.6716
E 204	.1430	.6315	.6789	.1434	.6306	.6779
H 276	.1447	.6195	.6718	.1437	.6190	.6713
E 392	.1432	.6266	.6757	.1436	.6263	.6754
H 488	.1444	.6193	.6714	.1438	.6191	.6712
E 1246	.1435	.6215	.6726	.1437	.6215	.6726
H 1414	.1441	.6192	.6712	.1438	.6192	.6711
ref.[11]	.1440	.6190	.6710			

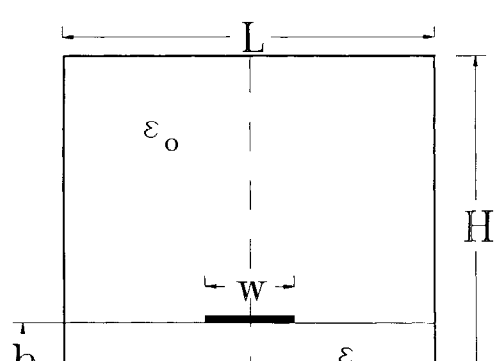

Fig. 8. Shielded microstrip line. $H = 12.7$ mm, $h = 1.27$ mm, $L = 12.7$ mm, $w = 1.27$ mm. $\varepsilon_r = 8.875$.

TABLE II
k_o (RAD/MM) FOR THE FUNDAMENTAL MODE ($\beta = 0.5$ RAD/MM) AND THE SECOND MODE ($\beta = 1$ RAD/MM) OF THE MICROSTRIP IN FIG. 8

Degrees of Freedom	Dominant Mode		Second Mode	
	REG.	SING.	REG.	SING.
221	.1958	.1934	.5523	.5460
454	.1951	.1934	.5499	.5485
883	.1946	.1932	.5489	.5481
1622	.1941	.1932	.5476	.5470
ref.[11]				
H	.1934			
E	.1953		.542	

IV. CONCLUSIONS

Edge elements achieve an adequate representation of E/H vectorial fields because only tangential continuity is imposed. Because of the correct representation of the null space of curl operator, spurious modes are confined in the zero eigenvalues and do not pollute the spectrum. However, conventional edge elements do not properly model the transverse field in the neighborhood of sharp edges. This leads to a slow convergence and a poor approximation of fields near to the edges.

In this paper, we have introduced a new edge element which, in addition to the usual advantages of edge elements (removal of spurious modes, ease of imposing boundary conditions), does a much better job of modeling the field and its curl near singularities. Analysis of some typical waveguides confirms that the results are improved in relation to conventional edge elements with the same number of degrees of freedom per element.

REFERENCES

[1] J. M. Gil and J. Zapata, "Efficient singular element for finite element analysis of quasi-TEM transmission lines and waveguides with sharp metal edges," *IEEE Trans. Microwave Theory Tech.*, vol. 42, pp. 92–98, Jan. 1994.

[2] ——, "A new scalar transition finite element for accurate analysis of waveguides with field singularities," *IEEE Trans. Microwave Theory Tech.*, vol. 43, pp. 1978–1982, Aug. 1995.

[3] J. P. Webb, "Finite element analysis of dispersion in waveguides with sharp metal edges," *IEEE Trans. Microwave Theory Tech.*, vol. 36, pp. 1819–1824, Dec. 1988.

[4] J.-F. Lee, D.-K. Sun, and Z. J. Cendes, "Full-wave analysis of dielectric waveguides using tangential vector finite elements," *IEEE Trans. Microwave Theory Tech.*, vol. 39, pp. 1262–1271, Aug. 1991.

[5] Z. Pantic-Tanner, D. R. Tanner, J. S. Savage, and A. F. Peterson, "The treatment of edge singularities in waveguiding problems using a finite element method based on edge elements," presented at the *AP-S/URSI Symp.*, Orlando, FL, 1995.

[6] J. Meixner, "The behavior of electromagnetic fields at edges," *IEEE Trans. Antennas Propagat.*, vol. AP-20, pp. 442–446, July 1972.

[7] A. Bossavit, "Edge-elements for scattering problems," *EDF Bulletin de la Direction des Etudes et Recherches, Serie C, Mathematiques, Informatique*, no. 2, pp. 175–191, 1989.

[8] M. Stern, "Families of consistent conforming elements with singular derivative fields," *Int. J. Numer. Methods Eng.*, vol. 14, pp. 409–421, 1979.

[9] M. Koshiba, K. Hayata, and M. Suzuki, "Finite-element formulation in terms of the electric-field vector for electromagnetic waveguide problems," *IEEE Trans. Microwave Theory Tech.*, vol. MTT-33, pp. 900–905, Oct. 1985.

[10] ——, "Improved finite-element formulation in terms of the magnetic field vector for dielectric waveguides," *IEEE Trans. Microwave Theory Tech.*, vol. MTT-33, pp. 227–232, Mar. 1985.

[11] P. T. S. Liu and J. P. Webb, "Analysis of 3-D microwave cavities using hierarchal vector finite elements," in *Proc. Inst. Elect. Eng. Microwave Antennas Propagat.*, vol. 142, pp. 373–378, Oct. 1995.

[12] R. Miniowitz and J. P. Webb, "Covariant-projection quadrilateral elements for the analysis of waveguides with sharp edges," *IEEE Trans. Microwave Theory Tech.*, vol. 39, pp. 501–505, Mar. 1991.

José Mª Gil received the Ingeniero de Telecomunicación and Ph.D. degrees from the Universidad Politécnica de Madrid, Madrid, Spain, in 1986 and 1993, respectively.

He is currently a full-time Associate Professor in the Departamento de Electromagnetismo y Teoría de Circuitos, Universidad Politécnica de Madrid. From August 1995 to February 1996, he was a Visiting Scientist at the Computational Analysis and Design Laboratory, Department of Electrical Engineering, McGill University, Montreal, P.Q., Canada. His main field of interest includes computer methods in electromagnetics, especially the application of the FEM, and interactions of electromagnetic fields with biological tissues.

Jon P. Webb (M'83) received the Ph.D. degree from Cambridge University, Cambridge, U.K., in 1981.

Since 1982, he has been a Professor in the Electrical Engineering Department, McGill University, Montreal, P.Q., Canada. His area of research is computer methods in electromagnetics, especially the application of the FEM.